Cell

Regulated Accumulation of Desmosterol Integrates Macrophage Lipid Metabolism and Inflammatory Responses

Nathanael J. Spann,[1,11] Lana X. Garmire,[2,11] Jeffrey G. McDonald,[5] David S. Myers,[6] Stephen B. Milne,[6] Norihito Shibata,[1] Donna Reichart,[1] Jesse N. Fox,[1] Iftach Shaked,[10] Daniel Heudobler,[1] Christian R.H. Raetz,[7,12] Elaine W. Wang,[9] Samuel L. Kelly,[9] M. Cameron Sullards,[9] Robert C. Murphy,[8] Alfred H. Merrill, Jr.,[9] H. Alex Brown,[6] Edward A. Dennis,[3] Andrew C. Li,[4] Klaus Ley,[10] Sotirios Tsimikas,[4] Eoin Fahy,[2] Shankar Subramaniam,[1,2,3] Oswald Quehenberger,[4] David W. Russell,[5] and Christopher K. Glass[1,4,*]

[1]Department of Cellular and Molecular Medicine
[2]Department of Bioengineering
[3]Department of Chemistry and Biochemistry
[4]Department of Medicine
University of California, San Diego, 9500 Gilman Drive, La Jolla, CA 92093-0651, USA
[5]Department of Molecular Genetics, UT Southwestern Medical Center, 5323 Harry Hines Boulevard, Dallas, TX 75390, USA
[6]Department of Pharmacology, Vanderbilt Institute of Chemical Biology, Vanderbilt University School of Medicine, 23rd Avenue South & Pierce, Nashville, TN 37232-6600, USA
[7]Department of Biochemistry, Duke University School of Medicine, Box 3711, DUMC, Durham, NC 27710, USA
[8]Department of Pharmacology, University of Colorado Denver, 12801 E. 17th Avenue, Mail Stop 8303, Aurora, CO 80045, USA
[9]Schools of Biology, Chemistry, and Biochemistry and the Parker H. Petit Institute for Bioengineering and Bioscience, Georgia Institute of Technology, Atlanta, GA 30332-0230, USA
[10]La Jolla Institute of Allergy and Immunology, 9420 Athena Circle Drive, La Jolla, CA 92037, USA
[11]These authors contributed equally to this work
[12]Deceased
*Correspondence: ckg@ucsd.edu
http://dx.doi.org/10.1016/j.cell.2012.06.054

SUMMARY

Inflammation and macrophage foam cells are characteristic features of atherosclerotic lesions, but the mechanisms linking cholesterol accumulation to inflammation and LXR-dependent response pathways are poorly understood. To investigate this relationship, we utilized lipidomic and transcriptomic methods to evaluate the effect of diet and LDL receptor genotype on macrophage foam cell formation within the peritoneal cavities of mice. Foam cell formation was associated with significant changes in hundreds of lipid species and unexpected suppression, rather than activation, of inflammatory gene expression. We provide evidence that regulated accumulation of desmosterol underlies many of the homeostatic responses, including activation of LXR target genes, inhibition of SREBP target genes, selective reprogramming of fatty acid metabolism, and suppression of inflammatory-response genes, observed in macrophage foam cells. These observations suggest that macrophage activation in atherosclerotic lesions results from extrinsic, proinflammatory signals generated within the artery wall that suppress homeostatic and anti-inflammatory functions of desmosterol.

INTRODUCTION

Macrophage foam cells are characterized by massive accumulation of lipid and contribute to all phases of atherosclerosis, ranging from the initial development of fatty streaks to the rupture of unstable plaques (Glass and Witztum, 2001; Rocha and Libby, 2009). Macrophages within atherosclerotic lesions are thought to acquire the foam cell phenotype through the constitutive uptake and degradation of native and modified lipoproteins via scavenger receptors and micropinocytosis (Goldstein et al., 1979; Krieger and Herz, 1994; Miller et al., 2003). Excess cholesterol delivered to the macrophage by these pathways must be either exported to extracellular acceptors via cholesterol efflux pathways or esterified for storage in cytoplasmic lipid droplets in order to prevent the cytotoxic effects associated with elevated free cholesterol within the endoplasmic reticulum (Tabas, 2010).

Many lines of evidence support the concept that inflammation plays a key role in the initiation, progression, and clinical complications of atherosclerosis (Glass and Witztum, 2001; Hansson et al., 2006; Rocha and Libby, 2009; Ross, 1993). Chemokines produced in response to inflammatory signals promote recruitment of monocytes/macrophages and other immune cells into the artery wall. These cells in turn secrete numerous factors, including cytokines, reactive oxygen species, and additional chemokines, that amplify inflammation and promote lesion development (Charo and Taubman, 2004; Hansson et al., 2006). Production of matrix metalloproteinases by macrophage

foam cells in advanced lesions is thought to contribute to weakening of the fibrous cap and an increased risk of plaque rupture and acute myocardial infarction (Galis et al., 1995; Hansson et al., 2006; Rocha and Libby, 2009).

A relationship also exists between circulating levels of low-density lipoprotein (LDL) cholesterol and inflammatory responses that promote atherosclerosis. Elevated LDL cholesterol levels are strongly correlated with risk for the development of clinically significant atherosclerosis in humans and with circulating markers of inflammation, such as C reactive protein (Blake and Ridker, 2003; Hansson et al., 2006). Similarly, animal models of atherosclerosis that are driven by genetic and/or dietary manipulations resulting in markedly elevated plasma cholesterol levels promote rapid lesion development and the attendant expression of inflammatory mediators (Getz and Reardon, 2006).

Despite these clear relationships, the mechanisms by which hypercholesterolemia induces the inflammatory response associated with atherosclerotic lesions remain poorly understood. Elevated levels of circulating LDL are thought to lead to increased rates of formation of oxidized LDL (oxLDL) and other modified forms of LDL in the artery wall (Steinberg, 2009). In addition to being a ligand for macrophage scavenger receptors, oxLDL contains numerous bioactive lipid species that can act on several cell types within the artery wall to induce the expression of proinflammatory mediators, including cytokines, chemokines, and adhesion molecules (Steinberg, 2009). OxLDL and other modified forms of LDL have been shown to exert inflammatory effects through several different pattern recognition receptors, including Toll-like receptors (TLR) (Choi et al., 2009; Chou et al., 2008; Xu et al., 2001). Increasing evidence supports roles for TLR 2 and 4 in promoting inflammation and atherosclerosis in mouse models and human lesions (Michelsen et al., 2004; Monaco et al., 2009; Mullick et al., 2008). In addition, macrophage uptake of cholesterol crystals has been shown to result in activation of the inflammasome (Duewell et al., 2010). Collectively, these findings suggest that hypercholesterolemia is directly linked to both foam cell formation and inflammation.

To further investigate the relationship between hypercholesterolemia, foam cell formation, and inflammation, we performed lipidomic and transcriptomic analyses of elicited peritoneal macrophages in wild-type (WT) or LDL receptor knockout (LDLR KO) mice fed either a normal-cholesterol, normal-fat (NCNF) diet or a high-cholesterol, high-fat (HCHF) ''Western'' style diet. The combination of the LDLR KO genotype and the HCHF diet results in the formation of macrophage foam cells in the elicited peritoneal macrophage population (Li et al., 2004). Analysis of macrophages from the above four experimental groups revealed massive reprogramming of the lipidome in response to both diet and genotype. These studies confirmed and extended prior knowledge regarding the roles of SREBP and LXR signaling in cholesterol and fatty acid homeostasis. Unexpectedly, peritoneal macrophage foam cells exhibited a strongly ''deactivated'' phenotype, with marked suppression of proinflammatory mediators that are normally characteristic of the inflammatory responses associated with atherosclerotic lesions. Many of these changes in gene expression and lipid metabolism appear to be related to the paradoxical accumulation of high levels of desmosterol, the last intermediate in the Bloch pathway of cholesterol biosynthesis.

RESULTS

Overview of the Elicited Macrophage Foam Cell Lipidome and Transcriptome

WT or LDLR KO mice were fed either a NCNF diet or a HCHF diet for 12 weeks to establish four experimental groups (WT-NCNF diet, WT-HCHF diet, KO-NCNF diet, and KO-HCHF diet). As expected, the combination of the HCHF diet and LDLR KO genotype resulted in a synergistic effect on serum lipid levels (Figure 1A). Elicited peritoneal macrophages (92%–96% F4/80-positive) were immediately prepared for analysis, thereby preserving in vivo gene expression and lipid profiles. Macrophages derived from LDLR KO mice fed the HCHF diet contained nearly 4-fold more total cholesterol than cells from WT mice fed the same diet (Figure 1B). Quantitative analysis of 245 lipid species revealed significant changes in nearly all major lipid classes (Figure 1C). Using a two-way ANOVA model, we found that 176 (72%) of the lipids analyzed were significantly affected by the HCHF diet, 133 (54%) by the LDLR KO genotype, and 114 (46%) by interactions between the HCHF diet and LDLR KO genotype (Table S1A available online). Many of the observed interactions (60%) were synergistic.

Parallel analysis of the macrophage transcriptome also demonstrated a synergistic effect of LDLR genotype and diet on gene expression (Figures 1D and 1E; Tables S1B–S1E). Using a cut-off threshold of 1.5-fold change and a false discovery rate (FDR) threshold of 0.05, we observed that the HCHF diet resulted in significantly more gene expression changes in LDLR KO mice than in WT mice. We also observed that more genes were downregulated than upregulated by the HCHF diet in both genotypes. Genes with functions related to blood vessel development, lipid transport, and extracellular matrix organization were over-represented in the upregulated gene sets identified in LDLR KO macrophages (Figure 1D; Tables S1B–S1E). As expected, genes associated with sterol biosynthesis were enriched in the set of downregulated genes. Unexpectedly, genes with functional annotations linked to inflammation, immunity, and defense response were the most highly over-represented genes in the downregulated gene set (Figure 1E; Tables S1B–S1E).

Alterations of Cholesterol Homeostasis in Macrophage Foam Cells

Cholesterol biosynthesis is mediated by a biochemical pathway, starting from acetyl-CoA (Figure 2A), whose encoding genes are primarily regulated by the transcription factor SREBP2. Elevated levels of cholesterol and certain oxysterols inhibit the proteolytic processing of SREBP2 (encoded by *Srebf2*), thereby reducing levels of the active transcription factor in the nucleus and resulting in downregulation of most of the enzymes in the biosynthetic pathway (Goldstein et al., 1979). Transcriptomic analysis confirmed that many enzymes of cholesterol synthesis, including *Hmgcs1*, *Hmgcr*, *Lss*, and *Dhcr24*, were downregulated by the HCHF diet, especially in LDLR KO mice (Figure 2B), with *Dhcr24* being the most suppressed transcript among the entire set of transcripts

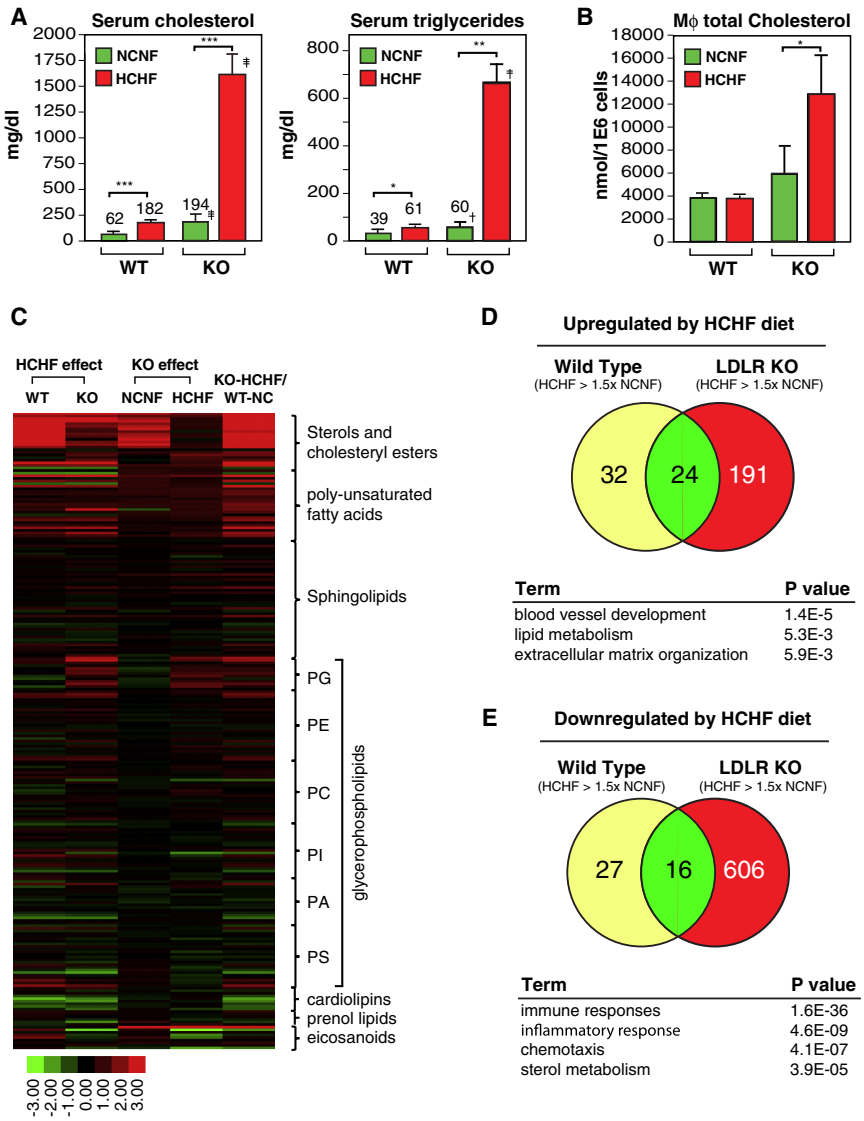

Figure 1. Overview of Global Effects of Diet and LDLR KO Genotype on the Lipidome and Transcriptome of Elicited Peritoneal Macrophages

(A) Serum cholesterol and triglyceride levels in elicited peritoneal macrophages from WT or LDLR KO mice fed either NCNF or HCHF diet. HCHF versus NCNF: ***p < 0.001, **p < 0.01, *p < 0.05. KO versus WT: ǂǂp < 0.001, ǂp < 0.01, +p < 0.05. Error bars represent standard error of the mean (SEM). n = 5.

(B) Total cellular cholesteryl esters in peritoneal macrophages derived from WT or LDLR KO mice fed either NCNF or HCHF diet. p value notations are the same as in (A) (n = 9).

(C) Heatmap of lipid changes in lipid categories. Log_2 of ratio values are used in each entry. Red shading indicates upregulation, and green indicates downregulation. For the subclasses under glycerophospholipids, the abbreviations are as follows: PG (glycerophosphoglycerols), PE (glycerophosphoethanolamines), PC (glycerophosphocholines), PI (glycerophosphoinositols), PA (phosphatidic acids), and PS (glycerophosphoserines).

(D) Venn diagram of upregulated genes and their overlap by HCHF diet > 1.5× in the transcriptome of WT and LDLR KO macrophages, and p values for selected gene ontology (GO) terms.

(E) Venn diagram of downregulated genes and their overlap by HCHF diet > 1.5× in the transcriptome of WT and LDLR KO macrophages, and p values for selected GO terms.

evaluated. LXRs provide a feedforward system for regulation of cholesterol homeostasis through activation of genes involved in cholesterol efflux, such as *Abca1* and *Abcg1* (Kennedy et al., 2001; Venkateswaran et al., 2000), and induction of the *Idol* gene that promotes degradation of the LDL receptor (Zelcer et al., 2009). These genes were significantly upregulated in macrophages elicited from mice fed the HCHF diet, especially from LDLR KO mice, as expected (Figure 2B).

The transcriptional activities of LXRs are positively regulated by specific oxysterols and sterols that include 24S-hydroxycholesterol (24-OHC), 25-hydroxycholesterol (25-OHC), 27-hydroxycholesterol (27-OHC), 24,25-epoxycholesterol (24,25-EC), and desmosterol (Yang et al., 2006; Chen et al., 2007; Janowski et al., 1996). Genetic studies have demonstrated that 24-OHC, 25-OHC, and 27-OHC are major oxysterols that regulate LXR activity in liver (Chen et al., 2007), but the oxysterol species that regulate LXRs in the context of macrophage foam cell formation have not been established. Surprisingly, desmosterol was by far the major LXR ligand to accumulate in peritoneal macrophage foam cells (Figure 2C). Significant increases in 24S-OHC, 25-OHC, and 27-OHC were also observed (Figures 2C and S2A), but the absolute amounts of these oxysterols were approximately 50-fold lower than the amount of desmosterol. Furthermore, genes encoding enzymes required for synthesis of 24-OHC, 25-OHC, and 27-OHC (*Cyp46a1, Ch25h*, and *Cp27a1*, respectively) were unchanged or downregulated in macrophage foam cells (Figure 2B). Based on the relative affinities of desmosterol, 24S-OHC, 25-OHC, and 27-OHC for LXRs (Yang et al., 2006) and the ability of desmosterol to suppress SREBP processing, these findings suggest that desmosterol is the dominant bioactive sterol in peritoneal macrophage foam cells.

To examine the potential relevance of this finding to macrophage foam cells in atherosclerotic lesions, human atherosclerotic lesions obtained during clinically indicated atherectomy of the lower extremities from three symptomatic patients with lifestyles limiting claudication were analyzed for sterols and oxysterols. This analysis indicated that relative levels of desmosterol significantly exceeded those of other known LXR ligands (Figures 2D and S1B), similar to the pattern observed in peritoneal macrophage foam cells.

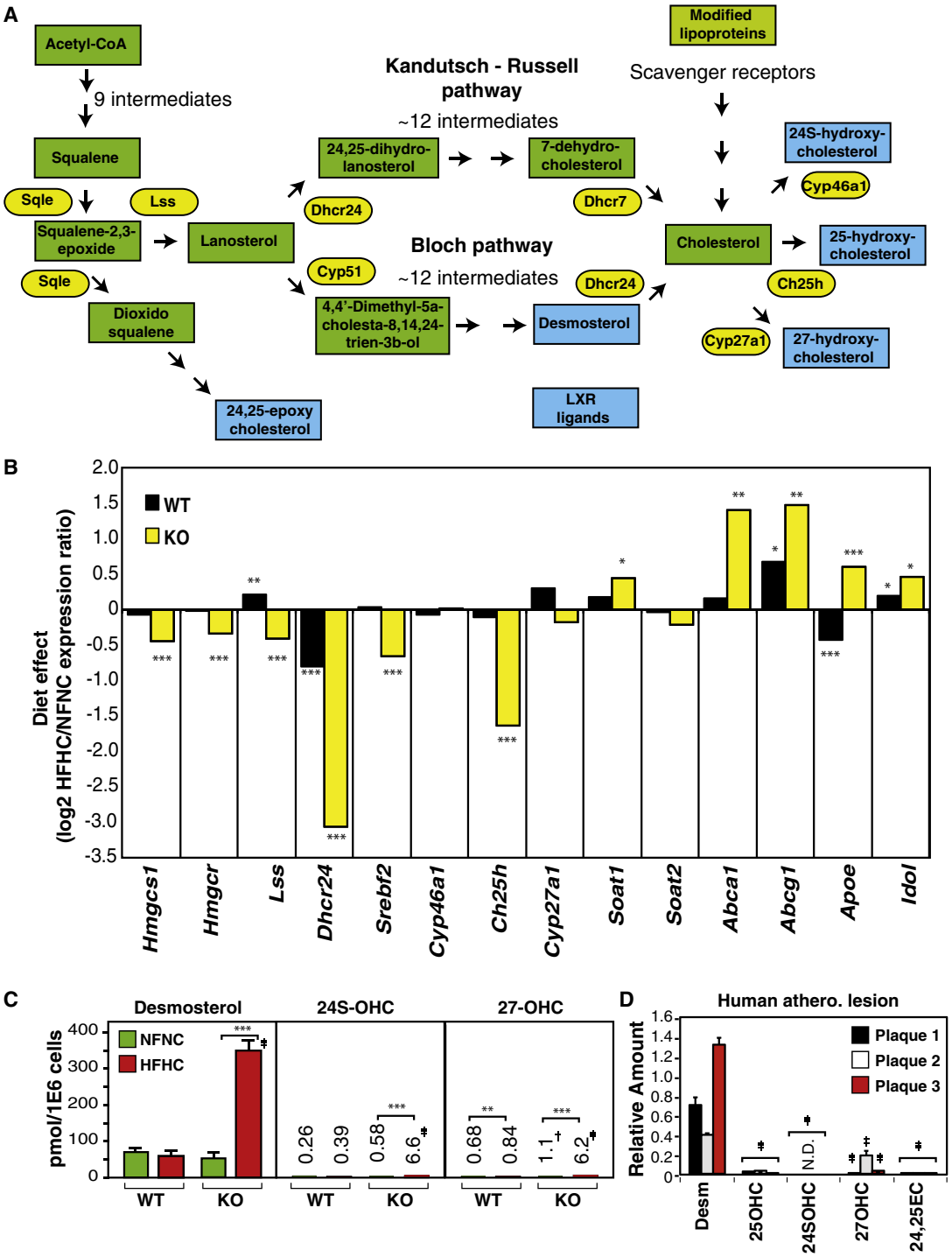

Figure 2. Foam Cell Formation Is Associated with Increased Cellular Content of Desmosterol

(A) A simplified scheme of cholesterol and oxysterol biosynthetic pathways. Selected lipid intermediates are labeled in green boxes, and important enzymes are labeled in yellow ellipses. Lipid species shown in blue boxes are LXR agonists.

(B) Effect of the HCHF diet on levels of mRNA transcripts of proteins involved in cholesterol homeostasis from WT and LDLR KO macrophages, as determined by microarray analysis. ***$p < 0.001$, **$p < 0.01$, *$p < 0.05$ ($n = 5$).

(C) Cellular levels of selected endogenous LXR ligands. p value notations are the same as in Figure 1A ($n = 9$).

(D) Levels of selected LXR ligands in human atherosclerotic lesions. Ligand levels per sample were normalized to cholestanol. Ligand versus desmosterol: ***$p < 0.001$, **$p < 0.01$, *$p < 0.05$.

Error bars represent SEM, and $n = 3$ unless otherwise indicated. See also Figure S1.

Altered Fatty Acid Metabolism in Macrophage Foam Cells

The HCHF diet induced numerous changes in saturated, monounsaturated, and polyunsaturated free fatty acids (FFAs), particularly in macrophages elicited from LDLR KO mice (Figure 1C; Table S1A). Among the most prominent of these changes were increases in 9Z-palmitoleic acid, recently suggested to be a "lipokine" capable of improving insulin sensitivity when injected intravenously in mice (Cao et al., 2008), and oleic acid, which is the dominant FFA incorporated into cholesterol esters (CE) (Figure 3A; Table S1A). Molecular species containing these fatty acids were also markedly increased in the cellular phospholipid pool, almost exclusively in the glycerophosphoglycerol (PG) fraction (Figures 1C and 3A).

Metabolic steps involved in the biosynthesis of palmitic, stearic, 9Z-palmitoleic, and oleic acids are indicated in Figure 3B, and the effects of diet on the expression of genes encoding the enzymes that catalyze these and other steps are indicated in Figure 3C. The most notable changes were diet-induced suppression of *Fads1* and *Fasn* expression in macrophages derived from LDLR KO animals and diet-induced increases in expression of *Acot1* and *Scd2* in macrophages derived from both WT and LDLR KO mice. The suppression of *Fasn* expression implies that there should be relatively little contribution of endogenous biosynthesis to palmitic acid levels. Palmitic acid, oleic acid, and stearic acid are major fatty acyl components of triglycerides in the HCHF diet, suggesting that increases in these macrophage FFAs are primarily due to hydrolysis of lipoprotein-derived triglyceride; however, the relative increase in oleic acid is significantly greater than that of palmitic acid, and 9Z-palmitoleic acid is not a significant fatty acid in the HCHF diet. These relationships suggest that the majority of 9Z-palmitoleic acid and a fraction of oleic acid are derived from the conversion of palmitic acid and stearic acid, respectively, due to upregulation of *Acot1/2* and *Scd1/2*.

Desmosterol Integrates LXR- and SREBP-Dependent Gene Expression

In addition to cooperating with SREBP2 to regulate cholesterol homeostasis, LXRs and SREBP1a and SREBP1c regulate fatty acid metabolism (Chen et al., 2007), providing a potential connection point at which desmosterol could integrate these distinct pathways. SREBP1a and 1c are derived by transcription from alternative promoters and preferentially drive the expression of genes involved in fatty acid biosynthesis, including *Fasn*, *Fads1*, *Fads2*, *Scd1*, and *Scd2*. The SREBP1c promoter is potently activated by synthetic LXR ligands (Repa et al., 2000), but the physiological relevance of LXR activation of this pathway in macrophages is unclear.

To investigate the ability of desmosterol to differentially regulate expression of genes involved in cholesterol and fatty acid metabolism through integration of LXR-dependent and SREBP-dependent mechanisms, gene expression was analyzed in elicited peritoneal macrophages treated with desmosterol, the synthetic LXR agonist GW3965, or a combination of desmosterol and GW3965. Due to the ability of desmosterol, but not GW3965, to suppress SREBP processing, this experimental design allows inferences to be made regarding the relative contributions of direct activation of LXR target genes (i.e., activation by GW3965 in the presence of desmosterol) and responses mediated through secondary activation of SREBP1c (i.e., GW3965-induced expression that is suppressed by desmosterol). Consistent with this hypothesis, we observed the expected desmosterol-specific suppression of the SREBP target gene *Dhcr24* (Figures 4A and S2A). Parallel chromatin immunoprecipitation (ChIP) experiments confirmed a desmosterol-specific reduction of SREBP2 binding at the *Dhcr24* sterol-response element (Figure 4B). Conversely, desmosterol and GW3965 treatment resulted in a similar level of induction of the LXR target gene *Abcg1* (Figure 4A), with desmosterol exerting these effects in a concentration- and LXR-dependent manner (Figure S2A). Genes involved in fatty acid biosynthesis exhibited more complex patterns of regulation. *Fasn* was selectively activated by GW3965, and this induction was almost completely abolished by cotreatment with desmosterol. This result is consistent with GW3965 inducing SREBP1c expression, which is required for *Fasn* activation. In contrast, *Srebf1*, *Acsl4*, and *Scd2* were strongly activated by GW3965 and less strongly but significantly activated by desmosterol in a concentration- and LXR-dependent manner (Figures 4A and S2A). Similar patterns of regulation were observed in desmosterol-treated human monocyte-derived macrophages (HMDMs) (Figure S2B).

Using a specific small interfering RNA (siRNA) to knock down SREBP1 expression, we confirmed a requirement for SREBP1 for effects of GW3965 on expression of *Scd2, Acsl4,* and *Fasn*, but not *Abcg1*, expression (Figures 4C and S2C). ChIP experiments demonstrated significant increases in SREBP1 occupancy of all target genes examined following treatment with GW3965, exemplified by *Scd2* and *Fasn* (Figure 4B). In contrast, treatment of cells with desmosterol resulted in reduced SREBP1 occupancy at these genes. Further, desmosterol increased LXR transcriptional activity as demonstrated by induction of luciferase reporter constructs driven by either the *Abca1* promoter or an LXR enhancer element located 10 kb upstream of the *Scd2* promoter (Heinz et al., 2010) (Figure 4D). Consistent with these findings, treatment of macrophages with desmosterol led to increased cellular content of both SCD2 protein (Figure S2D) and its products oleic and 9Z-palmitoleic acid (Figure 4E).

Desmosterol Is Generated in Response to Cholesterol Loading

The accumulation of desmosterol in the context of foam cell formation was surprising given the observed suppression of the cholesterol biosynthetic pathway. To determine the effects of cholesterol loading on LXR ligand synthesis, we incubated cholesterol-starved peritoneal macrophages with cholesterol delivered in ethanol and quantified sterols and oxysterols by mass spectrometry. Unesterified desmosterol was by far the dominant LXR ligand observed in these experiments, but total levels were similar in cholesterol-starved (522 ± 62 pmol/10^6 cells) and cholesterol-loaded cells (482 ± 18 pmol/10^6 cells) (Figure S3A). We therefore considered the possibility that an increase in desmosterol arising from cholesterol accumulation might be obscured in cholesterol-starved cells in which the cholesterol biosynthetic pathway is induced. Consistent with

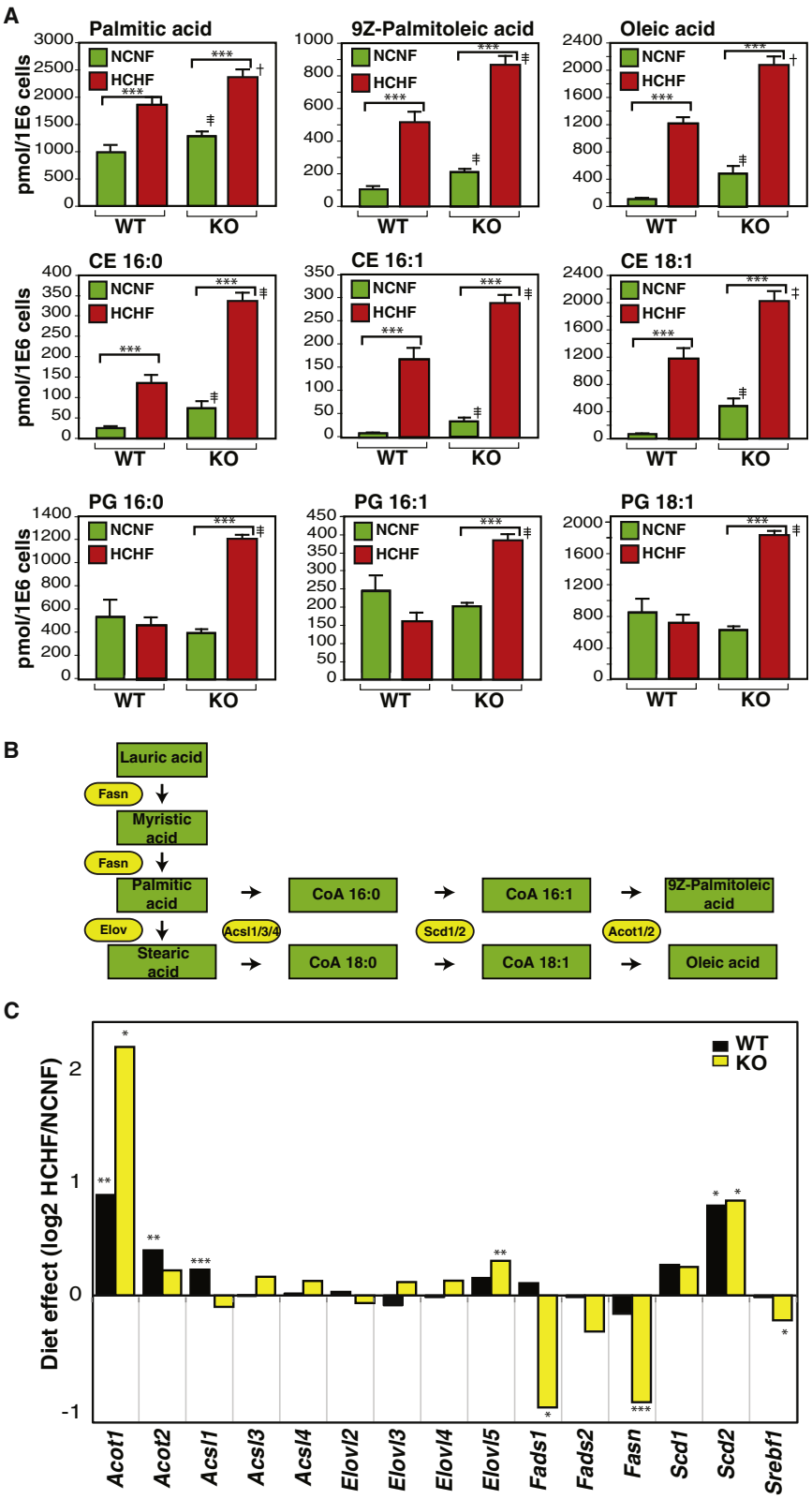

Figure 3. Foam Cell Formation Is Associated with Altered Fatty Acid Metabolism

(A) Cellular content of the indicated free fatty acids, cholesterol esters (CE), and glycerophosphoglycerols (PG) in peritoneal macrophages from WT and LDLR KO mice fed either NCNF or HCHF diet. p value notations are the same as in Figure 1A (n = 8–9).

(B) Scheme for biosynthesis of 9Z-palmitoleic acid and oleic acid. Selected lipid intermediates are labeled in green boxes, and enzymes are labeled in yellow ellipses.

(C) Effect of the HCHF diet on levels of selected mRNA transcripts encoding proteins involved in fatty acid metabolism from WT and LDLR KO macrophages, as determined by microarray analysis. ***p < 0.001, **p < 0.01, *p < 0.05.

Error bars represent SEM, and n = 5 unless otherwise indicated.

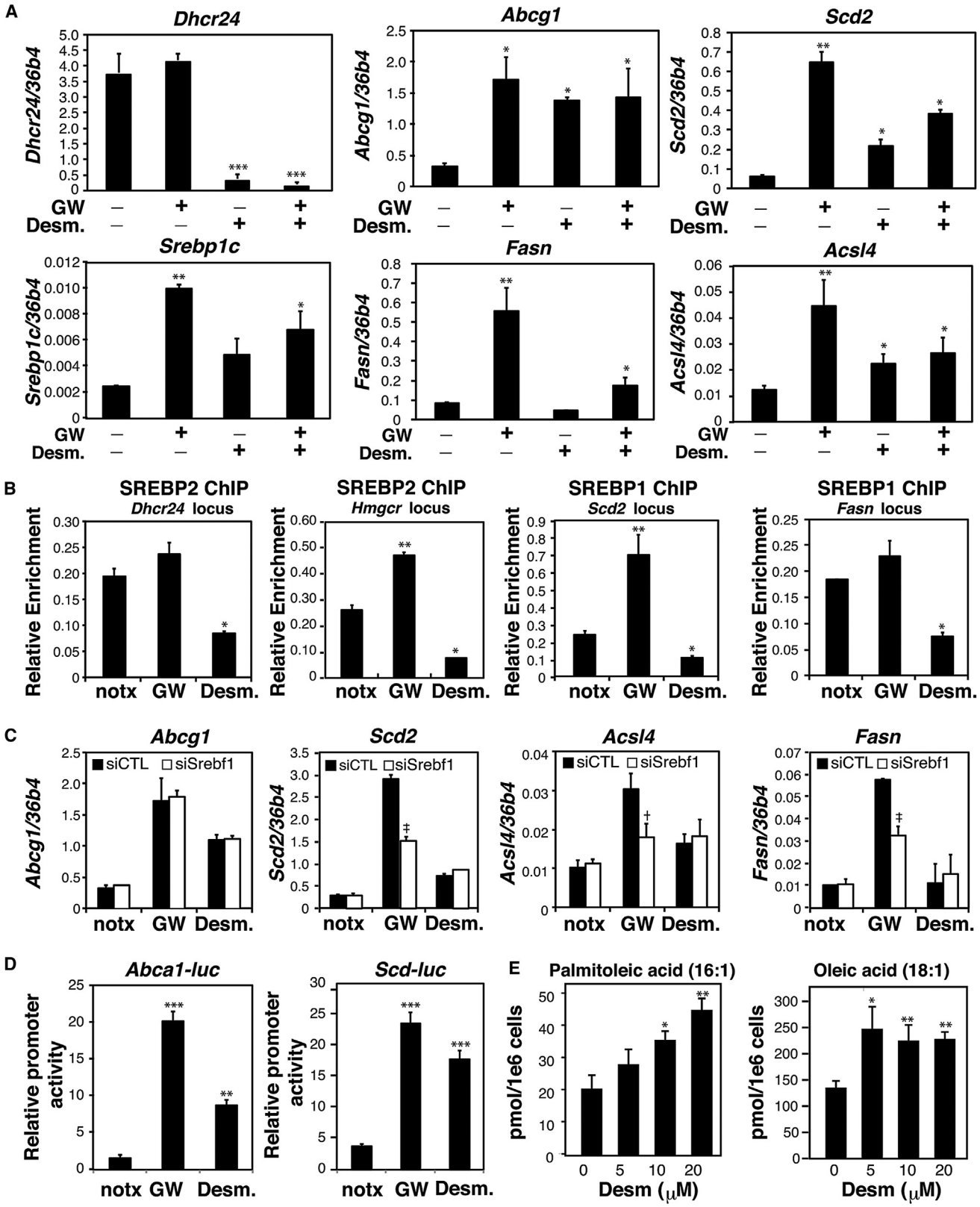
A
Dhcr24
Dhcr24/36b4
Abcg1
Abcg1/36b4
Scd2
Scd2/36b4
Srebp1c
Srebp1c/36b4
Fasn
Fasn/36b4
Acsl4
Acsl4/36b4
GW
Desm.
B
SREBP2 ChIP
Dhcr24 locus
Hmgcr locus
SREBP1 ChIP
Scd2 locus
Fasn locus
Relative Enrichment
notx GW Desm.
C
Abcg1
Scd2
Acsl4
Fasn
siCTL siSrebf1
D
Abca1-luc
Scd-luc
Relative promoter activity
E
Palmitoleic acid (16:1)
Oleic acid (18:1)
pmol/1e6 cells
Desm (μM)

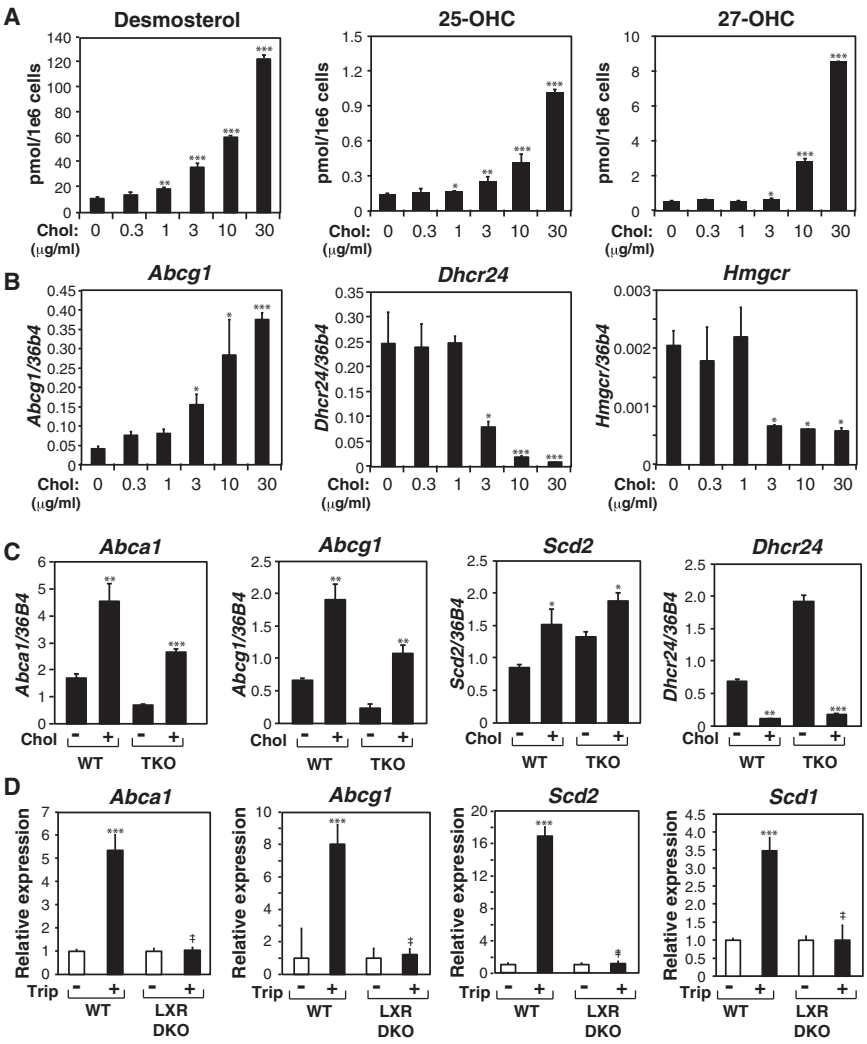

Figure 5. Desmosterol Accumulation and Function in Response to Cholesterol Loading of Primary Macrophages In Vitro

(A) LC-MS analysis of the effect of cholesterol loading of cholesterol-starved peritoneal macrophages on media content of desmosterol, 25-OHC, and 27-OHC.

(B) Effect of cholesterol loading on *Abcg1, Dhcr24*, and *Hmgcr* expression in the peritoneal macrophages used for analysis in (A).

(C) Effect of cholesterol loading on expression of *Abca1*, *Abcg1*, *Scd2*, and *Dhcr24* in WT peritoneal macrophages and TKO peritoneal macrophages deficient for *Cyp46a1*, *Ch25h*, and *Cyp27a1*.

For (A)–(C), ***p < 0.001, **p < 0.01, *p < 0.05 versus control. n = 2.

(D) Effect of triparanol inhibition of DHCR24 enzyme activity on the indicated LXR and SREBP target genes in WT and LXRα/β double knockout (LXR DKO) peritoneal macrophages. ***p < 0.001 versus control. ‡‡p < 0.001, ‡‡p < 0.01 DKO versus WT.

Error bars represent SD, and n = 3 unless otherwise indicated. See also Figure S3.

this possibility, macrophages cultured in the presence of 10% serum (i.e., not cholesterol starved) exhibited a lower basal level of free desmosterol (339 ± 6 pmol/10^6 cells) that increased (to 502 ± 44 pmol/10^6 cells, $p < 0.05$) upon cholesterol loading (Figure S3A).

The observation that desmosterol was the major LXR ligand in cholesterol-starved cells, in which LXR target genes are suppressed, suggests that this intermediate is preferentially utilized for cholesterol biosynthesis under these conditions and not accessible to LXRs. Unexpectedly, treatment of cholesterol-starved macrophages with increasing concentrations of free cholesterol, ranging from 0.3 μg/ml to 30 μg/ml, resulted in a marked dose-dependent increase in desmosterol in the medium (Figure 5A). Concentrations of 25-OHC and 27-OHC also increased in the medium in response to cholesterol loading, but at much lower levels (Figure 5A). Notably, expression levels of LXR target genes, such as *Abcg1* (Figure 5B), were closely correlated with desmosterol levels in the medium. Similar results were obtained in cholesterol-loaded HMDMs (Figures S3B and S3C).

To investigate whether the LXR pathway can respond to cholesterol accumulation independently of oxysterol production, cholesterol-loading experiments were performed to compare WT macrophages and triple knockout (TKO) macrophages derived from mice lacking the major enzymes responsible for production of 24-OHC, 25-OHC, and 27-OHC (*Cyp46a1*, *Ch25h*, and *Cyp27a1*). Basal expression levels of *Abca1* and

Figure 4. Desmosterol Coordinately Regulates LXR- and SREBP-Dependent Gene Expression and Induces Synthesis of Palmitoleic and Oleic Acid in Macrophages

(A) Quantitative PCR (qPCR) analysis of indicated mRNA transcripts in peritoneal macrophages treated with GW3965, desmosterol, or both.

(B) ChIP assay of SREBP at sterol-response elements that control the expression of the *Dhcr24, Scd2, Fasn*, and *Hmgcr* genes in cholesterol-depleted peritoneal macrophages under control, GW3965, or desmosterol treatment (6 hr). n =2.

(C) Effect of *Srebf1* knockdown on the expression of genes involved in cholesterol and fatty acid metabolism in peritoneal macrophages under lipid-depleted, desmosterol-treated, or GW3965-treated conditions. ‡‡p < 0.001, ‡p < 0.01, +p < 0.05 versus siCTL.

(D) Effect of GW3965 and desmosterol treatment on induction of indicated LXR reporter constructs in RAW264.7 cells.

(E) LC-MS analysis of the effects of desmosterol on cellular contents of 9Z-palmitoleic and oleic acid in peritoneal macrophages.

For (A), (B), (D), and (E), ***p < 0.001, **p < 0.01, *p < 0.05 versus control. Error bars represent standard deviation (SD), and n = 3 unless otherwise indicated.. See also Figure S2.

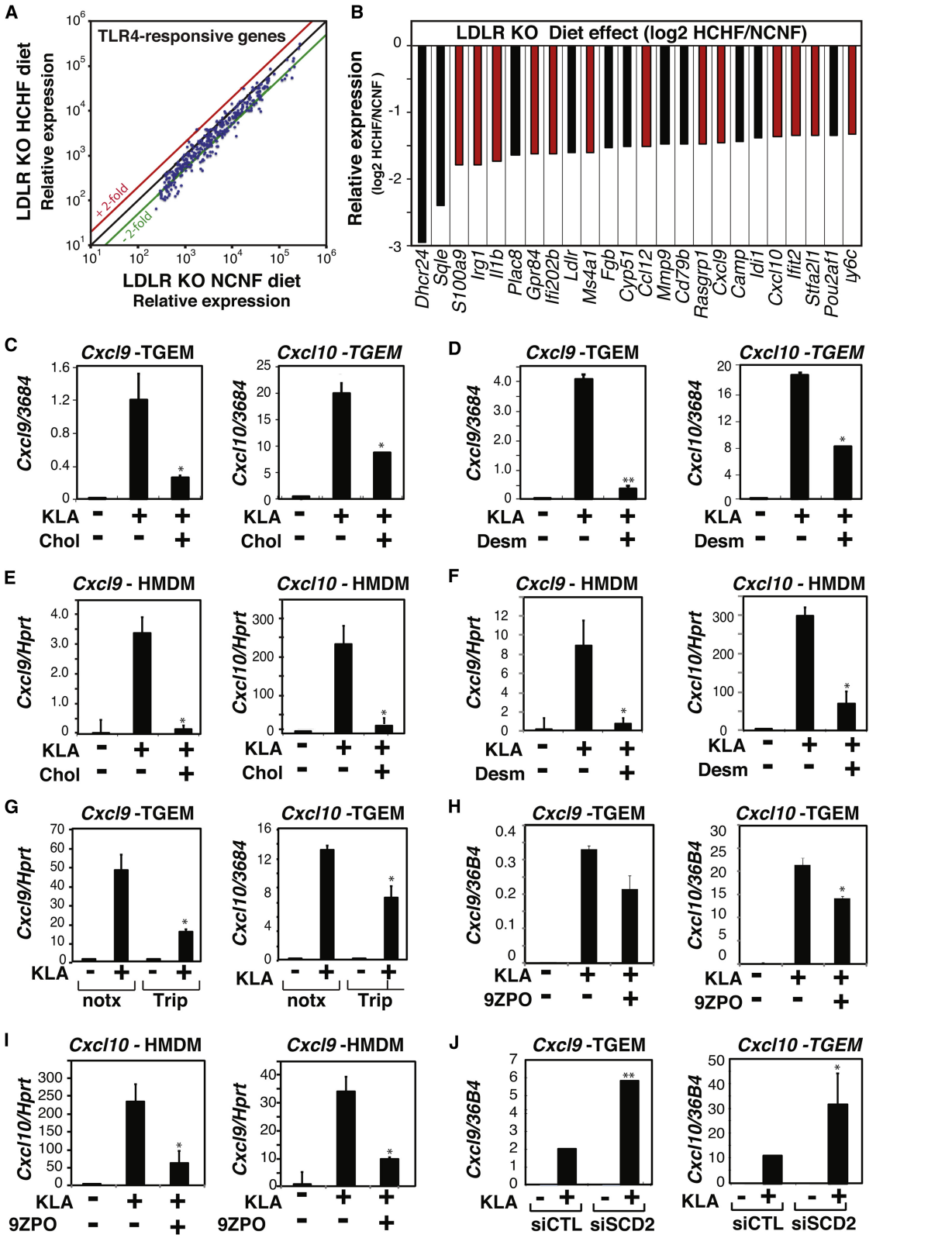

Figure 6. Desmosterol Inhibits Inflammatory Gene Expression

(A) TLR4 target genes are suppressed in macrophages derived from LDLR KO mice fed a HCHF diet. Relative expression of the 200 most highly induced TLR4 target genes in WT macrophages are plotted for LDLR KO macrophages under HCHF and NCNF diet conditions.

Abcg1 were reduced in cholesterol-starved TKO macrophages as compared to WT macrophages, consistent with 24*S*-OHC, 25-OHC, and/or 27-OHC playing roles in regulating basal LXR activity under these conditions (Figure 5C). However, cholesterol loading of TKO macrophages still resulted in a robust activation of *Abca1* and *Abcg1* (Figure 5C), with the fold-change in gene expression being similar to that of WT macrophages. As desmosterol is the only other significant LXR ligand produced in response to cholesterol loading, these results provide genetic evidence that this sterol activates the LXR program of gene expression in response to excess cholesterol. Although cholesterol loading strongly suppressed *Dhcr24* expression in both WT and TKO macrophages, this condition resulted in a further increase in *Scd2* expression (Figure 5C and S2D), consistent with the ability of *Scd2* to be positively regulated by an LXR-dependent, SREBP1-independent mechanism (Figure S3D).

The cholesterol biosynthetic pathway bifurcates at lanosterol (Figure 2A), with DHCR24 catalyzing the first step of the Kandutch-Russell pathway (lanosterol to 24,25-dihydrolanosterol) and the last step of the Bloch pathway (desmosterol to cholesterol). Thus, preferential downregulation of *Dhcr24* would be expected to result in accumulation of desmosterol as long as the upstream steps of the cholesterol biosynthetic pathway are not completely suppressed. Quantitative PCR analysis of gene expression in the same cells used for sterol and oxysterol analyses indicated that *Dhcr24* and *Hmgcr* are both downregulated at between 1 and 3 μg/ml of added cholesterol (Figure 5B). However, *Dhcr24* becomes profoundly repressed (>95%), whereas *Hmgcr* messenger RNA (mRNA) remains expressed at approximately 30% of the levels observed in cholesterol-starved cells. Although additional posttranslational mechanisms regulating enzymatic activity may also influence desmosterol levels, the concentration-dependent changes in *Dhcr24* mRNA were in good agreement with the concentration-dependent increases in media desmosterol and LXR target gene activation (Figures 5A, 5B, S3B, and S3C).

To determine whether reduction of DHCR24 activity is sufficient to activate LXRs, we inhibited the enzyme by treating macrophages with triparanol (Avigan et al., 1960) and then evaluated LXR-dependent gene expression. Triparanol-mediated inhibition of enzyme activity led to an LXR-dependent induction of target genes (Figure 5D), consistent with the observation that triparanol treatment increases desmosterol levels in Chinese hamster ovary (CHO) cells (Yang et al., 2006). Similarly, siRNA-mediated reduction of Dhcr24 levels resulted in significant accumulation of desmosterol in macrophages (Figures S3E and S3F).

Foam Cell Formation and Inflammatory Gene Expression

Perhaps the most unexpected finding related to macrophage foam cell formation in the peritoneal cavity was the broad suppression of genes that are normally induced by proinflammatory stimuli. Notably, a majority of the genes that are highly induced (>4-fold at 6 hr) in macrophages by the TLR4-specific agonist Kdo2 lipid A (KLA) (Raetz et al., 2006) were downregulated in macrophage foam cells derived from LDLR KO mice fed the HCHF diet (Figure 6A). The most strongly suppressed inflammatory-response genes at an FDR < 0.05 are illustrated in Figure 6B and include *Il1b*, *Cxcl9*, and *Cxcl10*. These findings suggested that cholesterol accumulation suppressed, rather than stimulated, signaling pathways responsible for the activation of these genes in macrophages. Consistent with this, cholesterol loading of thioglycollate-elicited macrophages inhibited activation of a subset of TLR4-responsive genes, exemplified by *Cxcl9* and *Cxcl10* (Figure 6C). In addition, pretreatment of macrophages with desmosterol resulted in a significant reduction of the KLA-mediated increases in expression of the *Cxcl9* and *Cxcl10* mRNAs (Figure 6D). The inhibitory effects of cholesterol loading and desmosterol treatment were also observed at the levels of the secreted proteins (Figure S4A). Similar effects were observed in HMDMs (Figures 6E and 6F) and for a significant subset of the TLR4-reponsive genes that were suppressed by the HCHF diet in elicited LDLR KO macrophages (Figure S5B), indicating that exogenous desmosterol is capable of recapitulating aspects of the deactivated phenotype exhibited by macrophage foam cells formed in vivo. In addition to suppressing TLR4-dependent gene expression, desmosterol also inhibited activation of responses to tumor necrosis factor alpha (TNF-α), Pam3 (TLR2 agonist), and poly(I:C) (TLR3 agonist) to variable extents, exemplified by Cxcl10 (Figure S4B).

To investigate whether endogenously produced desmosterol can exert an anti-inflammatory response, we treated macrophages with triparanol to inhibit DHCR24 enzyme activity or used specific siRNAs to knock down DHCR24 mRNA expression (Figure S4C). Each of these perturbations that cause accumulation of endogenous desmosterol resulted in reduced responsiveness of *Cxcl9* and *Cxcl10* to KLA (Figures 6G and S4D). Similarly, inhibition of DHCR24 enzyme activity in HMDMs led to reduced responses of *Cxcl9* and *Cxcl10* to KLA (Figure S4E).

The finding of increased levels of 9Z-palmitoleic acid in macrophage foam cells and the report that this fatty acid can function as an insulin-sensitizing lipokine (Cao et al., 2008) led us to directly evaluate the lipid's effects on macrophage activation. Overnight incubation of elicited peritoneal macrophages or

(B) Relative expression levels of the 24 most downregulated genes in LDLR KO macrophages from mice fed the HCHF versus NCNF diet. TLR4-responsive genes highlighted in red. Results are plotted as $\log_2$-fold change. $p < 0.001$ ($n = 9$).
(C) Effect of cholesterol loading on KLA-induced expression of *Cxcl10* and *Cxcl9* genes in peritoneal macrophages.
(D) Effect of desmosterol treatment on KLA-induced expression of *Cxcl9* and *Cxcl10* genes in peritoneal macrophages.
(E) Effect of cholesterol loading on KLA-induced expression of *Cxcl9* and *Cxcl10* genes in HMDMs.
(F) Effect of desmosterol treatment on KLA-induced expression of *Cxcl9* and *Cxcl10* genes in HMDMs.
(G) Effect of triparanol inhibition of DHCR24 enzyme activity on the KLA responsiveness of *Cxcl9* and *Cxcl10* genes in peritoneal macrophages. See also Figure S4.
(H) Effect of 9Z-palmitoleic acid (9Z-PO) treatment on KLA responses of *Cxcl9* and *Cxcl10* genes in peritoneal macrophages.
(I) Effect of knockdown of *Scd2* (72 hr) on KLA responses of *Cxcl9* and *Cxcl10* genes in peritoneal macrophages. $n = 2$.
(J) Effect of 9Z-palmitoleic acid (9Z-PO) treatment on KLA responses of *Cxcl9* and *Cxcl10* genes in HMDMs.
For (C)–(J), $^{**}p < 0.01$, $^{*}p < 0.05$ versus KLA or siCTL-KLA. Error bars represent SD, and $n = 3$ unless otherwise indicated. In all panels where indicated, TGEM refers to thioglycollate-elicited macrophages, and HMDM refers to HMDMs.

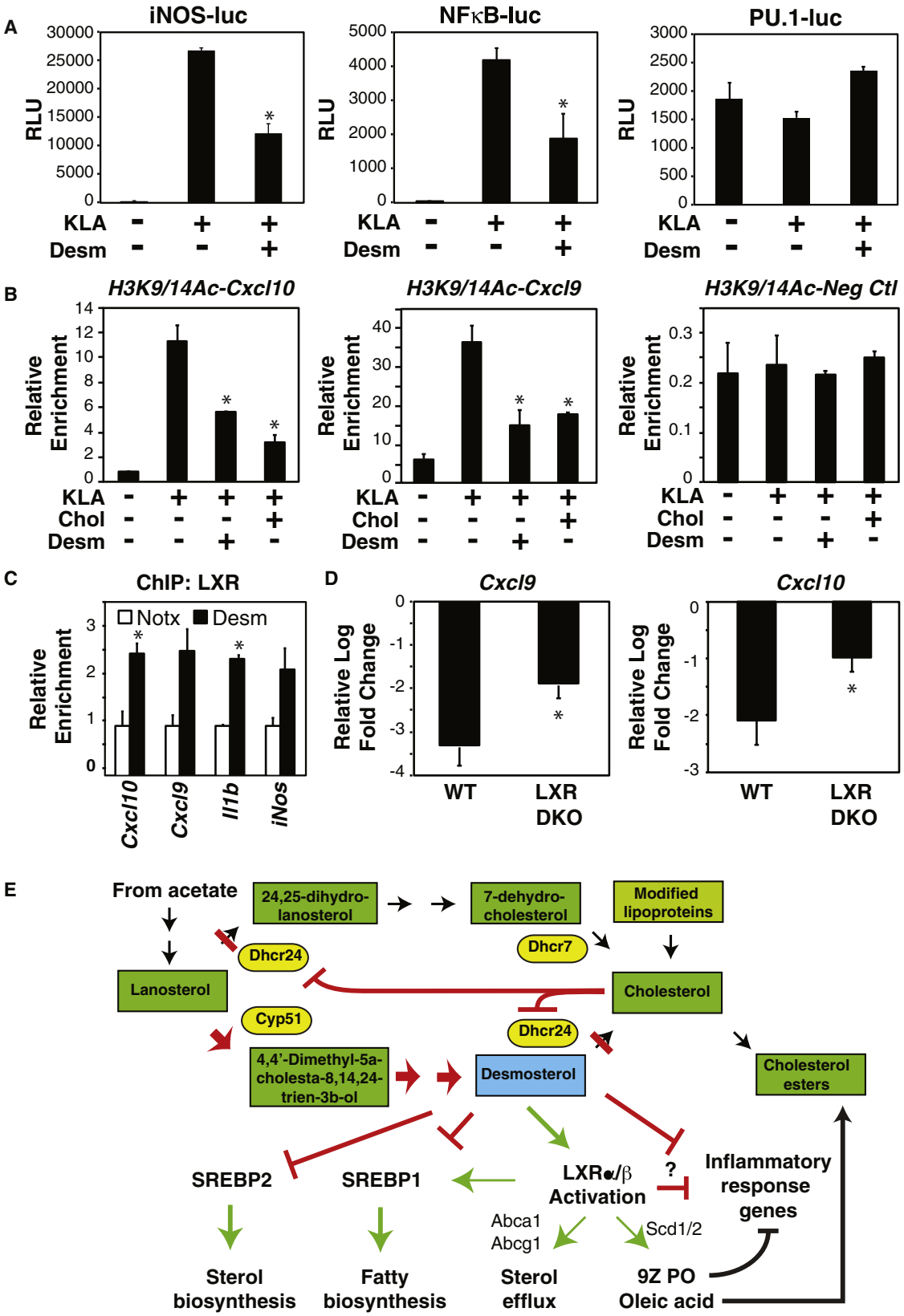
A
iNOS-luc
NFκB-luc
PU.1-luc
RLU
KLA
Desm
B
H3K9/14Ac-Cxcl10
H3K9/14Ac-Cxcl9
H3K9/14Ac-Neg Ctl
Relative Enrichment
KLA
Chol
Desm
C
ChIP: LXR
Notx
Desm
Relative Enrichment
Cxcl10
Cxcl9
Il1b
iNos
D
Cxcl9
Cxcl10
Relative Log Fold Change
WT
LXR DKO
E
From acetate
24,25-dihydro-lanosterol
7-dehydro-cholesterol
Modified lipoproteins
Dhcr24
Dhcr7
Lanosterol
Cholesterol
Cyp51
Dhcr24
4,4'-Dimethyl-5a-cholesta-8,14,24-trien-3b-ol
Desmosterol
Cholesterol esters
SREBP2
SREBP1
LXRα/β Activation
?
Inflammatory response genes
Abca1
Abcg1
Scd1/2
Sterol biosynthesis
Fatty biosynthesis
Sterol efflux
9Z PO Oleic acid

HMDMs with 9Z-palmitoleic acid blunted activation of several TLR4-inducible genes, including *Cxcl9* and *Cxcl10* (Figures 6H and 6I). Conversely, siRNA knockdown of *Scd2* (Figure S4F) resulted in increased responses of these genes (Figure 6J).

To investigate mechanisms by which desmosterol inhibits TLR4 signaling, we assessed the effect of desmosterol treatment on luciferase reporter genes driven by the TLR4-responsive iNOS promoter (Ricote et al., 1998), multimerized NF-κB sites, or multimerized binding sites for the macrophage lineage-determining factor PU.1. Desmosterol treatment inhibited KLA activation of the iNOS and NF-kB-driven promoters but had no effect on expression of the PU.1-element-driven promoter (Figure 7A). Although these results suggested that desmosterol inhibited NF-κB-dependent gene expression at the level of transcription, ChIP experiments indicated that desmosterol treatment did not prevent binding of the p65 subunit of NF-κB to target response elements (Figure S5A).

Previous studies have shown that LXRs can inhibit TLR4 signaling in macrophages by binding to and preventing the removal of NCoR/histone-deacetylase corepressor complexes at TLR4-responsive regulatory elements (Ghisletti et al., 2007). This repression mechanism does not alter p65 binding but prevents signal-dependent histone acetylation required for gene activation. We therefore assessed the effect of desmosterol treatment on local acetylation status of histone H3 lysine 9/14 (H3K9/14Ac), a histone modification that is associated with gene activation (Roh et al., 2007). Desmosterol inhibited KLA-mediated H3K9/14 acetylation at regulatory elements of the *Cxcl9* and *Cxcl10* genes (Figure 7B). In addition, desmosterol treatment promoted recruitment of LXR to *Cxcl9*, *Cxcl10*, *iNos*, and *Il1b* regulatory elements (Figure 7C), consistent with the presence of NCoR at these sites under basal conditions (Barish et al., 2012). Accordingly, desmosterol-mediated repression of a number of KLA-responsive genes was compromised in LXR DKO macrophages (Figure 7D). However, desmosterol continued to exert partial repressive effects on inflammatory-response genes even in LXR DKO macrophages (Figure 7D), indicating additional LXR-independent mechanisms.

DISCUSSION

Desmosterol Integrates Feedforward and Feedback Regulation of Cholesterol Homeostasis

Due to their normal physiological roles in phagocytosis of apoptotic and necrotic cells, macrophages must both suppress SREBP processing and upregulate LXR-dependent efflux mechanisms to maintain cholesterol homeostasis. Although free cholesterol is a potent suppressor of SREBP processing by binding to SCAP, it does not directly activate LXRs. The present studies provide evidence that, rather than converting cholesterol to an oxysterol, desmosterol (an intermediate in the cholesterol biosynthetic pathway) is the dominant LXR ligand generated during foam cell formation in vivo. Studies of the structural basis for the ability of the dietary sterol stigmasterol to activate LXRs led to the finding that desmosterol, although not previously considered to be a physiologically important LXR ligand, is an effective activator of LXR (Yang et al., 2006). Furthermore, these studies demonstrated that desmosterol bound directly to LXRs, induced recruitment of coactivators, and activated LXR target genes in WT but not LXR KO cells. Although the binding affinity of desmosterol for LXRs is about one-fifth that of the most potent oxysterol ligand, 24, 25-EC, (Yang et al., 2006), desmosterol was present in peritoneal macrophage foam cells at ~20-fold higher levels than the combined concentrations of 24,25-EC, 24S-OHC, 25-OHC, and 27-OHC, consistent with this sterol being the dominant LXR ligand in this setting. Desmosterol was also the dominant LXR ligand in cholesterol-loaded HMDMs and human atherosclerotic lesions. These findings suggest that the molecular and biochemical pathway for desmosterol production identified in mouse peritoneal macrophage foam cells is likely to be relevant to cholesterol homeostasis in human macrophages. It will therefore be of considerable interest to determine whether the relative activity of this pathway is affected by natural genetic variation and influences susceptibility to development of atherosclerosis.

An important caveat in drawing conclusions from measurements of cellular sterols and oxysterols is that their subcellular compartmentalization is not known. The dramatic differences in the amount of desmosterol released into the medium in cholesterol-starved versus cholesterol-loaded macrophages suggest that desmosterol is dedicated to cholesterol biosynthesis under cholesterol-starved conditions but becomes accessible to LXRs in cholesterol-loaded cells. This observation also likely explains the increase in LXR target genes in macrophages obtained from HCHF-fed WT mice despite relatively constant levels of total cellular desmosterol and other LXR ligands (Figure 2C). Defining the underlying mechanisms that regulate access of desmosterol to LXRs will be an important question for future investigation.

Because the cholesterol biosynthetic pathway is suppressed in the setting of foam cell formation, the marked increase in desmosterol (an intermediate in the cholesterol biosynthetic

Figure 7. Desmosterol Inhibits Inflammatory Gene Expression by LXR-Dependent and LXR-Independent Mechanisms

(A) Effect of desmosterol treatment on KLA induction of relative luciferase activities of indicated reporter constructs in RAW264.7 cells. *p < 0.01 versus KLA.

(B) ChIP analysis of effect of desmosterol treatment on KLA-induced H3K9/14 acetylation (H3K9/14Ac) at promoter regions of desmosterol-repressed *Cxcl9* and *Cxcl10* genes in peritoneal macrophages. Negative control (Neg Ctl) refers to genomic region lacking H3K9/14Ac enrichment. *p < 0.05 versus KLA. n = 2.

(C) ChIP analysis of LXR recruitment to desmosterol-repressed loci of the *Cxcl9, Cxcl10, IL1b*, and *iNos* genes in peritoneal macrophages treated with either vehicle (Notx) or desmosterol for 6 hr. Relative enrichments are presented as % input of LXR ChIP normalized to IgG control. *p < 0.05 versus control. n = 2.

(D) qPCR analysis of the effect of desmosterol treatment on KLA response of *Cxcl9* and *Cxcl10* genes in WT and LXRα/β DKO (LXR DKO) macrophages. *p < 0.05 versus WT. Results are plotted as $\log_2$-fold change. Error bars represent SD, and n = 3 unless otherwise indicated.

(E) Model for mechanisms by which foam cell formation induces desmosterol accumulation, leading to integration of cholesterol and fatty acid metabolism and suppression of inflammatory gene expression.

Error bars represent SD. See also Figure S5.

pathway) was unexpected. We provide evidence that this apparent paradox can be explained by the extreme sensitivity of *Dhcr24* to sterol-mediated suppression. DHCR24 is strategically placed as the first step of the Kandutsch-Russell pathway, mediating conversion of lanosterol to 24,25-dihydrolanosterol, and as the last step of the Bloch pathway, mediating conversion of desmosterol to cholesterol. Our findings are consistent with a model in which the relative activity of DHCR24 relative to upstream enzymes in the cholesterol biosynthetic pathway is preferentially inhibited by excess cholesterol. As a consequence, flux through the cholesterol biosynthetic pathway is reduced but not eliminated, leading to the accumulation of desmosterol, the activation of LXRs, and further suppression of SREBP processing via Insig/SCAP-dependent mechanisms (Figure 7E). This coordinated regulatory response integrates both the feedforward and feedback arms of cholesterol homeostasis.

Roles of Desmosterol in Integration of Fatty Acid Homeostasis

Although the target genes of SREBPs and LXRs involved in cholesterol homeostasis are virtually mutually exclusive, SREBPs and LXRs target a highly overlapping set of genes involved in fatty acid biosynthesis. Although further studies will be required to fully understand the functional interactions between LXRs and SREBP1c at genes involved in fatty acid metabolism in macrophages, our findings clearly indicate that desmosterol is able to activate a subset of SREBP1 target genes, exemplified by *Scd1*, *Scd2*, and *Ascl4*, despite inhibiting SREBP1 binding to response elements in these genes. Each of these genes is also a direct LXR target (Heinz et al., 2010), suggesting that LXR activation is sufficient to drive their expression. The present studies suggest that this *Scd2* plays a primary role in mediating increases in levels of 9Z-palmitoleic and oleic acids in peritoneal macrophage foam cells, whereas the de novo biosynthesis of saturated fatty acids is suppressed (Figure 7E). This metabolic adaptation may be physiologically important in that oleic acid is by far the major fatty acyl chain incorporated into CE in macrophages recovered from both WT and LDLR KO mice.

Roles of Desmosterol in the Deactivated Macrophage Phenotype

Perhaps the most unexpected finding of these studies was the observation that macrophage foam cell formation is associated with a deactivated, rather than activated, gene expression profile. Numerous mechanisms are known that function to counter-regulate inflammatory responses within macrophages and other cell types. Among these, LXRs have been demonstrated to suppress inflammatory-response genes in a gene-specific manner through transrepression and other mechanisms (A-Gonzalez et al., 2009; Ghisletti et al., 2007; Joseph et al., 2003). The present studies provide evidence that desmosterol contributes to the deactivated phenotype of peritoneal macrophage foam cells in both an LXR-dependent and LXR-independent manner (Figure 7E). It will be of interest to define mechanisms responsible for LXR-independent repression mechanisms.

The deactivated phenotype of peritoneal macrophage foam cells implies that the acquisition of a proinflammatory phenotype in the context of atherosclerotic lesions is dependent on extrinsic proinflammatory stimuli within the artery wall. Such stimuli would include inflammatory mediators derived from endothelial cells and other cells in the artery wall (Charo and Taubman, 2004; Glass and Witztum, 2001; Hansson et al., 2006), uptake of cholesterol crystals (Duewell et al., 2010), and exposure to debris from apoptotic and necrotic cells (Tabas, 2010). Intriguingly, not all lesion macrophages exhibit features of classical activation, and there is evidence for considerable phenotypic variation based on expression of cell-surface markers (Johnson and Newby, 2009; Kadl et al., 2010; Tacke et al., 2007). Specific macrophage foam cell subpopulations that exhibit anti-inflammatory and atheroprotective features have been identified. In particular, recent fluorescence-activated cell sorting (FACS) analysis of lesion macrophage foam cell subpopulations revealed that roughly 22% of these cells exhibited features of ''M2'' or ''alternatively activated'' macrophages (Kadl et al., 2010).

The present findings also raise the question of whether the pathway for generation of desmosterol or its intracellular distribution are impaired in atherosclerotic lesion macrophages, as this would be predicted to limit LXR-dependent cholesterol efflux mechanisms, reduce conversion of palmitic acid to 9Z-palmitoleic acid, and compromise other anti-inflammatory effects of desmosterol. Although efforts to inhibit late stages of the cholesterol biosynthetic pathway as a means of reducing circulating cholesterol levels were curtailed by the complication of cataract formation (Kirby, 1967), the present studies provide evidence that the strategy of feedback suppression of *Dhcr24* is used by macrophage foam cells to increase endogenous desmosterol. This response in turn coordinately regulates the functions of LXRs and SREBPs to enable appropriate homeostatic responses to elevated levels of cholesterol and inhibits inflammatory responses (Figure 7E). These findings therefore provide impetus for further characterization and development of synthetic desmosterol-like molecules as the basis of new therapeutic interventions in cardiovascular disease.

EXPERIMENTAL PROCEDURES

Mice

Male WT C57BL6 or LDL receptor KO mice (Jackson Laboratory) were fed a NCNF diet or a HCHF diet (Harlan Teklad, catalog # 96121 including 21% milk fat and 1.25% cholesterol) for 12 weeks in an IACUC-approved animal facility. Cells were harvested from the peritoneal cavity 4 days after intraperitoneal (i.p.) administration of 3% thioglycollate medium. Cells were immediately counted, aliquoted, pelleted, and sent for cDNA microarray analysis and lipid measurement. For all other experiments, primary cells were isolated from male 6- to 8-week-old C57BL6 mice (Charles River Laboratories).

Cell Culture

Mouse thioglycollate-elicited macrophages and bone marrow-derived macrophages were obtained and cultured as described previously (Heinz et al., 2010). For various ligand treatments, cells were in Phenol-red free RPMI-1640 (Invitrogen) supplemented with either 10% heat-inactivated FBS (Hyclone) or 10% lipid-deficient FBS (Hyclone) for 24 hr before treatment, then treated with either 1 μM GW3965, 0.25–20 μM desmosterol, or 0.3–30 μg/ml cholesterol for 12–24 hr. Fifty micromoles of mevalonate and 10 μM Mevastatin (Sigma) were added to media in desmosterol-response experiments. For TLR repression studies, cells were cultured in medium containing Phenol-red free RPMI-1640 (Invitrogen) with either heat-inactivated

FBS (Hyclone) or lipid-deficient FBS (Hyclone) for 24 hr, then pretreated with either 20–30 μM desmosterol, 50 μg/ml cholesterol, 5 μM triparanol, or 50–100 μM 9Z-palmitoleic acid for 18 hr. Cells were stimulated with Pam3CSK4 (300 ng/ml), polyI:C (50 ng/ml), LPS (100 ng/ml), TNF-α (30 ng/ml), or KLA (100 ng/ml) for 6 hr. See Extended Experimental Procedures for additional details.

RNA Analysis

Total RNA was purified and analyzed by microarray and quantitative PCR as previously described (Ghisletti et al., 2007). Either 1 μl of complementary DNA (cDNA) or ChIP DNA was used for quantitative PCR with gene- or locus-specific primers (primer sequences are indicated in Table S2). See Extended Experimental Procedures for details of microarray analysis.

Lipid Measurements

Three separate experiments (biological replicates) and three technical replicates were carried out, and to measure lipid species, liquid chromatography-mass spectrometry (LC-MS) measurements were performed following detailed protocols available online: http://www.lipidmaps.org/protocols/index.html.

Raw lipid data are available at http://www.lipidmaps.org/data/results/foam/foam.html.

ChIP

For ChIP of SREBP and LXR, 4×10^7 macrophages were used per ChIP, which was performed as described previously (Reed et al., 2008). For ChIP of p65 and H3K9/14Ac, 2×10^7 macrophages were used per ChIP, as described previously (Heinz et al., 2010).

siRNA Knockdown

Thioglycollate-elicited macrophages were transfected with nonspecific (NS) control or indicated SMARTpool siRNAs (Dharmacon) using Deliver X transfection reagent (Panomics) according to the manufacturer's instructions. For SREBP1 siRNA experiments, 48 hr post-transfection, cells were treated for 24 hr with vehicle (DMSO), 1 μM GW3965, or 10 μM desmosterol. For *Scd2* and *Dhcr24* siRNA experiments, 48 hr post-transfection, cells were treated for 6 hr with vehicle (PBS) or 100 ng/ml KLA.

Reporter Gene Activity Assays

Transfections of RAW264.7 cells were performed as described previously (Heinz et al., 2010). For KLA-response studies, at 48 hr post-transfection, cells were treated with either 30 μM desmosterol or 100 μM 9Z-palmitoleic acid for 18 hr, followed by 100 ng/ml KLA for 8 hr. For activation experiments, cells were treated with either 1 μM GW3965 or 10 μM desmosterol for 24 hr. Relative light units (RLU) were given as transformed ratio of firefly luciferase to β-galactosidase.

Bioinformatics and Statistical Analysis

Microarray data were analyzed by GeneSpring GX 7.3.1. A small number of genes specific to B1 cells in the peritoneal macrophage preparations were eliminated from the list of statistically significant genes. Lipids with at least five detectable values were tested by two-way ANOVA models to calculate p values under the HCHF diet effect, LDLR KO effect, and their interaction.

SUPPLEMENTAL INFORMATION

Supplemental Information includes Extended Experimental Procedures, five figures, and two tables and can be found with this article online at http://dx.doi.org/10.1016/j.cell.2012.06.054.

ACKNOWLEDGMENTS

These studies were primarily supported by NIH grant GM U54 069338 to the LIPID MAPS Consortium. Additional support was provided by NIH grants PO1 HC088093 and P01 DK074868. N.J.S. was supported by an NIH training grant. We thank Hanna Lesch for critical comments, L. Bautista for assistance with preparation of the manuscript, and Dr. Peter Tontonoz for providing LXR DKO mice for macrophage isolation.

Received: January 22, 2012
Revised: May 21, 2012
Accepted: June 12, 2012
Published: September 27, 2012

REFERENCES

A-Gonzalez, N., Bensinger, S.J., Hong, C., Beceiro, S., Bradley, M.N., Zelcer, N., Deniz, J., Ramirez, C., Díaz, M., Gallardo, G., et al. (2009). Apoptotic cells promote their own clearance and immune tolerance through activation of the nuclear receptor LXR. Immunity *31*, 245–258.

Avigan, J., Steinberg, D., Thompson, M.J., and Mosettig, E. (1960). Mechanism of action of MER-29, an inhibitor of cholesterol biosynthesis. Biochem. Biophys. Res. Commun. *2*, 63–65.

Barish, G.D., Yu, R.T., Karunasiri, M.S., Becerra, D., Kim, J., Tseng, T.W., Tai, L.J., Leblanc, M., Diehl, C., Cerchietti, L., et al. (2012). The Bcl6-SMRT/NCoR cistrome represses inflammation to attenuate atherosclerosis. Cell Metab. *15*, 554–562.

Blake, G.J., and Ridker, P.M. (2003). C-reactive protein and other inflammatory risk markers in acute coronary syndromes. J. Am. Coll. Cardiol. *41* (4, Suppl S), 37S–42S.

Cao, H., Gerhold, K., Mayers, J.R., Wiest, M.M., Watkins, S.M., and Hotamisligil, G.S. (2008). Identification of a lipokine, a lipid hormone linking adipose tissue to systemic metabolism. Cell *134*, 933–944.

Charo, I.F., and Taubman, M.B. (2004). Chemokines in the pathogenesis of vascular disease. Circ. Res. *95*, 858–866.

Chen, W., Chen, G., Head, D.L., Mangelsdorf, D.J., and Russell, D.W. (2007). Enzymatic reduction of oxysterols impairs LXR signaling in cultured cells and the livers of mice. Cell Metab. *5*, 73–79.

Choi, S.H., Harkewicz, R., Lee, J.H., Boullier, A., Almazan, F., Li, A.C., Witztum, J.L., Bae, Y.S., and Miller, Y.I. (2009). Lipoprotein accumulation in macrophages via toll-like receptor-4-dependent fluid phase uptake. Circ. Res. *104*, 1355–1363.

Chou, M.Y., Hartvigsen, K., Hansen, L.F., Fogelstrand, L., Shaw, P.X., Boullier, A., Binder, C.J., and Witztum, J.L. (2008). Oxidation-specific epitopes are important targets of innate immunity. J. Intern. Med. *263*, 479–488.

Duewell, P., Kono, H., Rayner, K.J., Sirois, C.M., Vladimer, G., Bauernfeind, F.G., Abela, G.S., Franchi, L., Nuñez, G., Schnurr, M., et al. (2010). NLRP3 inflammasomes are required for atherogenesis and activated by cholesterol crystals. Nature *464*, 1357–1361.

Galis, Z.S., Sukhova, G.K., Kranzhöfer, R., Clark, S., and Libby, P. (1995). Macrophage foam cells from experimental atheroma constitutively produce matrix-degrading proteinases. Proc. Natl. Acad. Sci. USA *92*, 402–406.

Getz, G.S., and Reardon, C.A. (2006). Diet and murine atherosclerosis. Arterioscler. Thromb. Vasc. Biol. *26*, 242–249.

Ghisletti, S., Huang, W., Ogawa, S., Pascual, G., Lin, M.E., Willson, T.M., Rosenfeld, M.G., and Glass, C.K. (2007). Parallel SUMOylation-dependent pathways mediate gene- and signal-specific transrepression by LXRs and PPARgamma. Mol. Cell *25*, 57–70.

Glass, C.K., and Witztum, J.L. (2001). Atherosclerosis. the road ahead. Cell *104*, 503–516.

Goldstein, J.L., Ho, Y.K., Basu, S.K., and Brown, M.S. (1979). Binding site on macrophages that mediates uptake and degradation of acetylated low density lipoprotein, producing massive cholesterol deposition. Proc. Natl. Acad. Sci. USA *76*, 333–337.

Hansson, G.K., Robertson, A.K., and Söderberg-Nauclér, C. (2006). Inflammation and atherosclerosis. Annu. Rev. Pathol. *1*, 297–329.

Heinz, S., Benner, C., Spann, N., Bertolino, E., Lin, Y.C., Laslo, P., Cheng, J.X., Murre, C., Singh, H., and Glass, C.K. (2010). Simple combinations of

lineage-determining transcription factors prime cis-regulatory elements required for macrophage and B cell identities. Mol. Cell *38*, 576–589.

Janowski, B.A., Willy, P.J., Devi, T.R., Falck, J.R., and Mangelsdorf, D.J. (1996). An oxysterol signalling pathway mediated by the nuclear receptor LXR alpha. Nature *383*, 728–731.

Johnson, J.L., and Newby, A.C. (2009). Macrophage heterogeneity in atherosclerotic plaques. Curr. Opin. Lipidol. *20*, 370–378.

Joseph, S.B., Castrillo, A., Laffitte, B.A., Mangelsdorf, D.J., and Tontonoz, P. (2003). Reciprocal regulation of inflammation and lipid metabolism by liver X receptors. Nat. Med. *9*, 213–219.

Kadl, A., Meher, A.K., Sharma, P.R., Lee, M.Y., Doran, A.C., Johnstone, S.R., Elliott, M.R., Gruber, F., Han, J., Chen, W., et al. (2010). Identification of a novel macrophage phenotype that develops in response to atherogenic phospholipids via Nrf2. Circ. Res. *107*, 737–746.

Kennedy, M.A., Venkateswaran, A., Tarr, P.T., Xenarios, I., Kudoh, J., Shimizu, N., and Edwards, P.A. (2001). Characterization of the human ABCG1 gene: liver X receptor activates an internal promoter that produces a novel transcript encoding an alternative form of the protein. J. Biol. Chem. *276*, 39438–39447.

Kirby, T.J. (1967). Cataracts produced by triparanol. (MER-29). Trans. Am. Ophthalmol. Soc. *65*, 494–543.

Krieger, M., and Herz, J. (1994). Structures and functions of multiligand lipoprotein receptors: macrophage scavenger receptors and LDL receptor-related protein (LRP). Annu. Rev. Biochem. *63*, 601–637.

Li, A.C., Binder, C.J., Gutierrez, A., Brown, K.K., Plotkin, C.R., Pattison, J.W., Valledor, A.F., Davis, R.A., Willson, T.M., Witztum, J.L., et al. (2004). Differential inhibition of macrophage foam-cell formation and atherosclerosis in mice by PPARalpha, beta/delta, and gamma. J. Clin. Invest. *114*, 1564–1576.

Michelsen, K.S., Wong, M.H., Shah, P.K., Zhang, W., Yano, J., Doherty, T.M., Akira, S., Rajavashisth, T.B., and Arditi, M. (2004). Lack of Toll-like receptor 4 or myeloid differentiation factor 88 reduces atherosclerosis and alters plaque phenotype in mice deficient in apolipoprotein E. Proc. Natl. Acad. Sci. USA *101*, 10679–10684.

Miller, Y.I., Chang, M.K., Binder, C.J., Shaw, P.X., and Witztum, J.L. (2003). Oxidized low density lipoprotein and innate immune receptors. Curr. Opin. Lipidol. *14*, 437–445.

Monaco, C., Gregan, S.M., Navin, T.J., Foxwell, B.M., Davies, A.H., and Feldmann, M. (2009). Toll-like receptor-2 mediates inflammation and matrix degradation in human atherosclerosis. Circulation *120*, 2462–2469.

Mullick, A.E., Soldau, K., Kiosses, W.B., Bell, T.A., 3rd, Tobias, P.S., and Curtiss, L.K. (2008). Increased endothelial expression of Toll-like receptor 2 at sites of disturbed blood flow exacerbates early atherogenic events. J. Exp. Med. *205*, 373–383.

Raetz, C.R., Garrett, T.A., Reynolds, C.M., Shaw, W.A., Moore, J.D., Smith, D.C., Jr., Ribeiro, A.A., Murphy, R.C., Ulevitch, R.J., Fearns, C., et al. (2006). Kdo2-Lipid A of Escherichia coli, a defined endotoxin that activates macrophages via TLR-4. J. Lipid Res. *47*, 1097–1111.

Reed, B.D., Charos, A.E., Szekely, A.M., Weissman, S.M., and Snyder, M. (2008). Genome-wide occupancy of SREBP1 and its partners NFY and SP1 reveals novel functional roles and combinatorial regulation of distinct classes of genes. PLoS Genet. *4*, e1000133.

Repa, J.J., Liang, G., Ou, J., Bashmakov, Y., Lobaccaro, J.M., Shimomura, I., Shan, B., Brown, M.S., Goldstein, J.L., and Mangelsdorf, D.J. (2000). Regulation of mouse sterol regulatory element-binding protein-1c gene (SREBP-1c) by oxysterol receptors, LXRalpha and LXRbeta. Genes Dev. *14*, 2819–2830.

Ricote, M., Li, A.C., Willson, T.M., Kelly, C.J., and Glass, C.K. (1998). The peroxisome proliferator-activated receptor-gamma is a negative regulator of macrophage activation. Nature *391*, 79–82.

Rocha, V.Z., and Libby, P. (2009). Obesity, inflammation, and atherosclerosis. Nat Rev Cardiol *6*, 399–409.

Roh, T.Y., Wei, G., Farrell, C.M., and Zhao, K. (2007). Genome-wide prediction of conserved and nonconserved enhancers by histone acetylation patterns. Genome Res. *17*, 74–81.

Ross, R. (1993). The pathogenesis of atherosclerosis: a perspective for the 1990s. Nature *362*, 801–809.

Steinberg, D. (2009). The LDL modification hypothesis of atherogenesis: an update. J. Lipid Res. Suppl. *50*, S376–S381.

Tabas, I. (2010). Macrophage death and defective inflammation resolution in atherosclerosis. Nat. Rev. Immunol. *10*, 36–46.

Tacke, F., Alvarez, D., Kaplan, T.J., Jakubzick, C., Spanbroek, R., Llodra, J., Garin, A., Liu, J., Mack, M., van Rooijen, N., et al. (2007). Monocyte subsets differentially employ CCR2, CCR5, and CX3CR1 to accumulate within atherosclerotic plaques. J. Clin. Invest. *117*, 185–194.

Venkateswaran, A., Laffitte, B.A., Joseph, S.B., Mak, P.A., Wilpitz, D.C., Edwards, P.A., and Tontonoz, P. (2000). Control of cellular cholesterol efflux by the nuclear oxysterol receptor LXR alpha. Proc. Natl. Acad. Sci. USA *97*, 12097–12102.

Xu, X.H., Shah, P.K., Faure, E., Equils, O., Thomas, L., Fishbein, M.C., Luthringer, D., Xu, X.P., Rajavashisth, T.B., Yano, J., et al. (2001). Toll-like receptor-4 is expressed by macrophages in murine and human lipid-rich atherosclerotic plaques and upregulated by oxidized LDL. Circulation *104*, 3103–3108.

Yang, C., McDonald, J.G., Patel, A., Zhang, Y., Umetani, M., Xu, F., Westover, E.J., Covey, D.F., Mangelsdorf, D.J., Cohen, J.C., and Hobbs, H.H. (2006). Sterol intermediates from cholesterol biosynthetic pathway as liver X receptor ligands. J. Biol. Chem. *281*, 27816–27826.

Zelcer, N., Hong, C., Boyadjian, R., and Tontonoz, P. (2009). LXR regulates cholesterol uptake through Idol-dependent ubiquitination of the LDL receptor. Science *325*, 100–104.